This is a post-refereed copy of the paper published in Electrochimica Acta 295 (2019) 333-339

Electrochemical determination of disulfoton using a molecularly imprinted poly-phenol polymer.

Bakhtiyar Qader[a,b], Mark Baron[b] , Issam Hussain[c], J.M. Sevilla[d], Robert P. Johnson[b], Jose Gonzalez-Rodriguez[b,*]

a Sulaimani Medicolegal institute, Qanat street, Sulaimani, Kurdistan regional government, Iraq.

b School of Chemistry, University of Lincoln, Brayford Pool, Lincoln LN6 7TS, UK. jgonzalezrodriguez@lincoln.ac.uk. Fax Number: +441522201109. Telephone: +441522886878.

c School of Life Sciences, University of Lincoln, Brayford Pool, Lincoln LN6 7TS, UK.

d Department of Physical Chemistry and Applied Thermodynamics, University of Cordoba, Marie Curie Building, Campus Universitario de Rabanales, Cordoba, Spain.

* Corresponding author

ABSTRACT: A simple, rapid and sensitive electrochemical method using a molecularly imprinted poly-phenol polymer for the analysis of disulfoton in model and real samples is demonstrated. A computational approach to molecularly imprinted polymer design and screening is followed using density functional (B3LYP) and Semi-Empirical Parameterized Model number 3 (PM3) models. The selected phenol monomer is electrochemically polymerized by cyclic voltammetry at a glassy carbon working electrode in the presence of a disulfoton template. The subsequent molecularly imprinted polymer sensor exhibits an oxidation peak at 1.13 V vs. Ag/AgCl in cyclic voltammetry with excellent linearity (r^2=0.9985) over the range 1-30 µM. The limit of detection for the DSN-MIP is 0.183 µM, compared to a limit of detection of 1.64 µM with cyclic voltammetry for the bare glassy carbon electrode. Intra- and inter-day assay precisions, expressed as relative standard deviation, are both found to be less than 7% overall. The developed molecularly imprinted polymer sensor is utilized to determine disulfoton in both spiked synthetic human plasma and human urine samples with recoveries ranging from 85.2% to 101.1%. The developed methods can be applied for measuring this toxicant in a real sample.

Keywords: Disulfoton; molecularly imprinted polymer; computational chemistry; electrochemistry; pesticides.

Introduction:

Organophosphorus compounds are the most commonly used pesticides in crop management. Disulfoton is an organophosphorus insecticide and acaricide that is used to eradicate pests in a wide range of crops. Annually, about 1.2 million pounds of disulfoton (DSN) are used to increase yield in the production of cotton, tobacco, potatoes, and wheat crops in the United States alone.[1] Despite its widespread use, disulfoton has also been classified as a neurotoxic and warfare agent and is highly toxic for human beings and aquatic animals. The toxicity arises from its inhibitory effect on acetylcholinesterase, leading to muscular spasm by accumulating acetylcholine neurotransmitters at the peripheral and central nerve systems.[2] If large amounts of disulfoton are utilized in crop spraying, there is the potential for percolation into the surface and groundwaters, contaminating the environment with disulfoton and its metabolites over time.[3] The primary route of disulfoton exposure in humans is dermal contact and inhalation, where it is subsequently rapidly distributed through the organs and tissue and carried by the blood circulatory system. The lethal concentration of disulfoton and its metabolites were determined in blood and urine in an elderly suicide victim as 360ng/mL. [4].

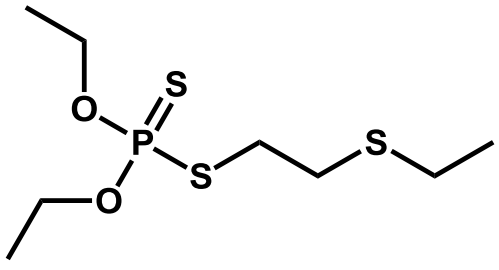

Figure 1: Chemical structure of Disulfoton

Although disulfoton does not accumulate in the organs and tissues, quickly changes to harmful substances, mainly through liver action in a metabolic oxidation of disulfoton to

disulfoton sulfoxide, disulfoton sulfone, demeton S-sulfoxide and demeton S-sulfone [5]. Disulfoton *in-vitro* studies found that the Cytochrome P450 and Flavin-containing monooxygenase enzymes in the presence of NADPH are responsible for the metabolism of disulfoton into Disulfoton sulfoxide, disulfoton sulfone, demeton S-sulfoxide and demeton S-sulfone as main metabolites. Nearly all by-products of disulfoton metabolism were excreted through urine, faeces and exhaled air in around 10 days as shown from recent animal studies. [6]

Different analytical methods have been developed for the determination of disulfoton including Spectro-fluorometry, [2] gas chromatography flame ionization detection (GC/FID), [1,3] high-performance liquid chromatography (HPLC), [7] liquid chromatography-mass spectrometry (LC-MS) [4] and gas chromatography-mass spectrometry (GC/MS) [8,9]. These methods are sensitive and robust but are expensive, have a long analysis time and the need of highly trained technicians and specialist equipment. In addition, they are not suitable for on-site detection and require complex sample pre-treatment steps in specialized facilities. [2]

The advantages of electrochemical methods over other techniques are that they are portable, fast, highly sensitive and reliable. Moreover sensitivity and selectivity of working electrodes can often be further increased using surface modification techniques. One such method is the use of molecularly imprinted polymers (MIPs), which are robust, cheap and present high performance and stability in a variety of conditions, including organic solvents at low and high pH. [10,11] Furthemore, MIPs have attracted considerable attention as a powerful analytical tool in the forensic field analysis due to their mechanical and thermal stability and portability. Molecular imprinted polymers can be easily prepared at low cost and using simple materials with good sensitivity, which enable MIP to be employed in

various fields, particularly in electrochemical sensors [12-14]. In order to generate a molecular imprinted polymer on the electrode surface, the functional monomers are mixed with a template of interest and a cross linker to form a polymer matrix. Subsequent removal of the template from the polymer matrix produces cavities complementary to the shape, size and functional groups of template. [15, 16] In the case of disulfoton, molecularly imprinted solid phase extraction has been applied for extraction of disulfoton from strawberry samples followed by GC-FID analysis. [17]

Nowadays computation studies are increasingly used for designing MIPs, where they can be used to predict a template-monomer interaction in pre-polymerization mixtures.[18-20] Density function theory (DFT) methods are adopted to select the best functional monomer in the MIP design and are based on the energy obtained in the monomer-template interaction. [18] For example, DFT has been successfully used to optimize and select functional monomers and suitable solvents for the production of MIPs using oxalic and hydrochlorothiazide templates [19, 20] and other pesticides [21].

To the best of our knowledge, no electrochemical method has been developed for the detection of disulfoton. In this article, we demonstrate the electrochemical analysis of disulfoton, initially on bare GC electrodes in real samples using cyclic voltammetry and differential pulse voltammetry techniques. Subsequently, we show that the limit of detection with cyclic voltammetry can be improved by a factor of ten through the use of a computationally selected molecularly imprinted polymer. Developed methods have been validated using GC/MS as reference method as a comparison.

Materials and methods

Chemical and reagents

Disulfoton, sodium chloride (NaCl), glacial acetic acid, potassium chloride (KCl), sodium perchlorate ($NaClO_4$), lithium perchlorate($LiClO_4$), sodium acetate buffer pH=5.2 (NaOAc), Britton Robinson (B-R) buffer phenol and artificial human plasma were obtained from Sigma-Aldrich (UK) and used without further purification. Acetonitrile (HPLC grade), phosphoric acid, Hydrochloric Acid and Potassium Hydroxide were all purchased from Fisher Scientific (UK). A Britton-Robinson buffer solution was prepared using phosphoric acid, glacial acetic acid and sodium chloride; the pH value was adjusted with NaOH and HCl. A 100 µM individual standard stock solution of disulfoton was prepared in acetonitrile and stored at -20 °C in amber bottles. All working solutions were freshly prepared from standard stock solution.

Fused silica (particle size 0.007 µm) and aluminium oxide (particle size 0.05 µm) were used for polishing the glassy carbon electrode (Sigma-Aldrich, UK).

Instruments and Apparatus

Voltammetric experiments were performed using a Metrohm 757 VA Computrace (Metrohm Ltd., UK), data processing was performed using Metrohm version 1.0 Ct757 software (Metrohm Ltd., UK). A conventional three electrode system consisting of a glassy carbon (GC) electrode, as the working electrode, a Ag/AgCl electrode, as reference electrode, and platinum as an auxiliary electrode were used for all the experiments (Metrohm Ltd., UK). Prior to running all experiments the GC electrode was polished to a mirror-like surface successively with activated aluminium oxide and 0.007 µm silica slurry. The electrode was thoroughly washed with water and then sonicated in acetonitrile for 5 minutes. Electrochemical experiments were carried out in a 50-mL voltammetric cell at

room temperature after an initial purging of the solution under nitrogen gas for 300 seconds.

For the validation of the samples, a Perkin Elmer GC model Clarus 500 equipped with an auto sampler and MS model Clarus 500 operated with Perkin Elmer TurboMass (2008) software were used. Standards and samples were run on an SUPELCO analytical, SLB-5m fused silica capillary column (30 m × 0.25 mm × 0.25 µm). Oven temperature started with an initial 60C˚ increasing at 20 C˚/min to 200 and held for 1 min. A final ramp of 10 °C min^{-1} was used to a final temperature of 280 °C. The carrier gas was helium at 1 mL/min and the injection volume was 1 µL. The transfer line temperature was held at 300 °C. Positive ionization was performed using an Electron Impact (EI+) source at 200 °C with electron energy of 70 eV and the multiplier was set to 350 V. The peaks were observed in total ion count (TIC) mode after 2 mins' solvent delay giving a total run time of 15 minutes.

Modification of a GC electrode with a poly-phenol imprinted polymer

The electro-polymerization was performed in an oxygen-purged electrolyte solution which contains 6 mM phenol, 2 mM disulfoton, and 100 mM $NaClO_4$ supporting electrolyte. at a clean glassy carbon electrode. The copolymerization of the Phenol and disulfoton was initiated by performing cyclic voltammetry in a potential range of 0 to 1.2 V vs Ag/AgCl at a scan rate of 0.05 V s^{-1} for 10 cycles. The disulfoton molecules were removed from the polymeric film by immersing the MIP electrode into a stirred mixture of acetic acid and acetonitrile at a ratio of 1:5 (v/v). Finally, the molecularly imprinted GC electrode was then dried under nitrogen gas. The non-imprinted polymer (NIP) was also prepared by following

the same electro-polymerization and template removal steps but without the presence of the template molecule, disulfoton, in the electrolyte mixture.

Computational approach

Quantum calculations were carried out using Spartan 14, V1.1.4 software. The electronic binding energies were calculated through Density Functional Theory (DFT) and the geometry optimization was performed at the B3LYP/6-31G level. Finally, the molar concentration ratio between template and monomer was studied using Semi-Empirical model (PM3). Using Spartan software, the chemical structure of the template (disulfoton), monomers and all template-monomer complexes were drawn (each chemical structure representing one molecule in the polymerisation solution) and calculations for the interaction between the different molecules and complexes created were performed to assess their stability and interaction energies.

Results and Discussion

Electrochemical behaviour of disulfoton

The oxidative voltammetric behaviour of disulfoton was studied by CV on a bare GC electrode. A well-defined oxidation peak was observed for disulfoton at potential 1.087 V vs. Ag/AgCl in a $NaClO_4$ supporting electrolyte. No peak was observed on the reverse scan, indicating the oxidation to be irreversible and suggesting a subsequent, rapid chemical reaction of the oxidative product. The influence of the pH on the disulfoton oxidation peak was examined with DPV in a Briton-Robinson buffer in the pH range 3.0-8.0. The peak current intensity was found to be pH dependent, with the highest current intensity response

for the disulfoton peak observed at pH 6, as shown in Fig. 2A. This indicated the optimal concentration for further studies.

To study the influence of the supporting electrolyte solution on the peak intensity, various buffers and supporting electrolytes at the same concentration (0.1 M) including potassium chloride (KCl), sodium perchlorate ($NaClO_4$), lithium perchlorate($LiClO_4$), sodium acetate buffer pH=5.2 (NaOAc), Britton Robinson (B-R) buffer (pH=6), and phosphate saline buffer, pH=6 (PSB) were investigated. The best intensity current was found for the sodium perchlorate solution shown in Fig 2B.

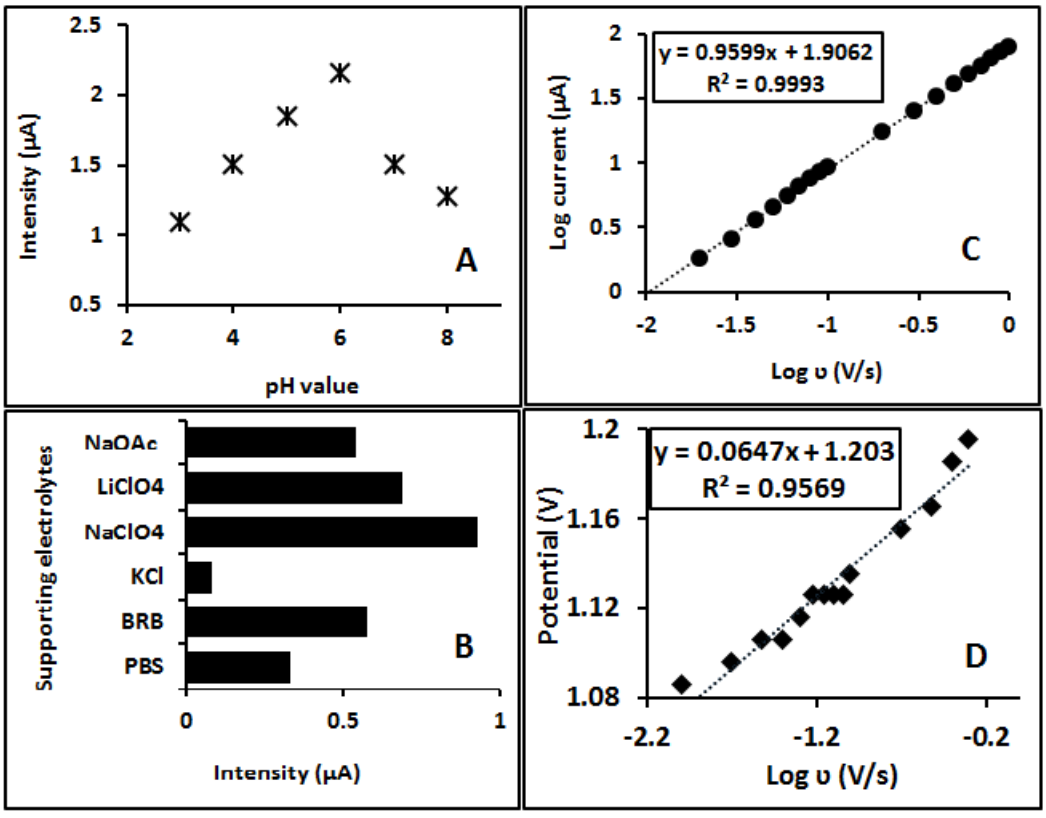

Figure 2: A) the anodic peak intensity against pH value at 20 µM disulfoton concentration; B) for Peak current response of 20 µM disulfoton in various supporting electrolytes; C) the value of logarithm of intensity versus vs logarithm of scan rates ranging from 10-1000 mV s^{-1} for 20 µM disulfoton anodic peak. D) Linear dependence of the peak potential of 20 µM disulfoton with the logarithm of scan rate.

The effect of scan rates (υ) on the disulfoton oxidation peak was also investigated within the range 10–1000 mV s^{-1}, and the peak potential was found to shift towards more negative values when the scan rate was decreased, confirming the irreversibility of the oxidation reaction. A plot of log (v) vs. peak intensity (log I_p) (Fig 2C) was found to be linear. The slope of the equation is close to the theoretical value of 1.0, which indicates that the reaction process at the electrode surface is adsorption-diffusion controlled [22]. The adsorption might be favoured by the interaction between disulfoton and the electrode surface as the low solubility of the molecule in water favours its absorption on a carbon-based surface. The presence of water also favours the possibility of an electrocatalytic reactions.

To assess the number of transferred electrons in the disulfoton oxidation reaction, a plot of peak potential (E_p) versus logarithm scan rate (log υ) in a sweep rate range 10-1000mV/s as seen in Fig 2D.

According to Laviron's equation [23] for an irreversible species:

$$E_p = E^{\circ} + \left(\frac{2.303RT}{\alpha nF}\right)\log\left(\frac{RTK^{\circ}}{\alpha nF}\right) + \left(\frac{2.303RT}{\alpha nF}\right) log\, \upsilon \qquad (1)$$

where α is the anodic electron transfer coefficient, R is the gas constant, T the temperature, F is Faraday's constant, K^o standard heterogeneous rate constant of the reaction, E^o formal redox potential, and n is the number of electrons.

Accordingly, the slope of Ep vs. log υ can be used for the calculation of αn [23]. From this calculation, αn was found to be equal to 0.90. This value yields a value of α is about 0.5 and an approximate number of electrons (n) of 2, corresponding to a bielectronic process. This biolectronic process is consistent with the previous metabolic pathways identified for disulfoton in the literature [5]. The suggested oxidation mechanism based on the available data is presented in Scheme 1. We propose that the oxidized product of disulfoton

undergoes subsequent and rapid hydrolysis to sulfenic acid and a second, non-electroactive fragment.

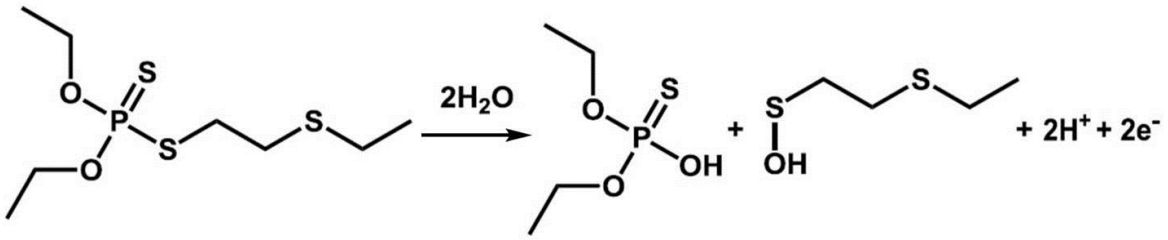

Scheme 1: Proposed mechanism for disufoton hydrolysis and oxidation and subsequent breakdown to a stable sulfonic acid species.

Analytical parameters

The anodic peak of disulfoton had a clear response when increasing concentrations of the analyte in the supporting electrolyte solution were used, as showed in Fig.3. The calibration curves showed good linear responses within the concentration range from 7 to 75 µM and from 5 to 75 µM with correlation coefficients of r^2=0.9993 and r^2=0.9991 using CV and DPV, respectively.

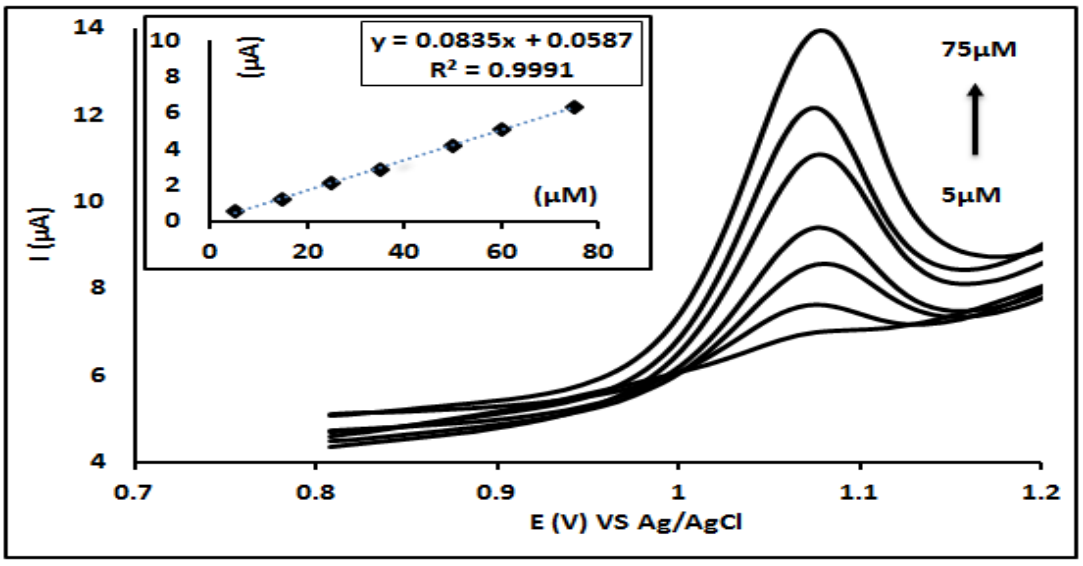

Figure 3: Differential pulse voltammogram for seven concentrations of disulfoton (5, 15, 25, 35, 45, 60, and 75) µM at bare GC electrode and regression line for calibrated disulfoton concentrations. Experimental conditions: pulse amplitude, 50mV; pulse time, 0.04s; and sweep rate, 25mV/s.

The limit of detection (LOD) was calculated using 3*S*/P and the limit of quantification (LOQ), and was calculated as 10 *S*/P, where *S* is the standard deviation of nine measurements of the lowest concentration and P is a slope of linear regression. Limits of detection were 1.64 µM and 0.443 µM for CV and DPV, respectively. Limits of quantification were 4.96 µM and 1.34 µM for CV and DPV, respectively. Thus, the sensitivity of the proposed method is nearly the same to those methods routinely used for the determination of disulfoton in human blood by LC/MS.[4] The recovered concentration of a 25 µM disulfoton solution analyzed by CV was found to be 23.2 µM (92.9%). The same solution analyzed by DPV yielded a concentration of 25.6 µM (102%). Intra-day precision (n=5) was found to be 2.68% and 4.91% (as %RSD) for CV and DPV, respectively. Inter-day precision (n=5) was found to be 11.4% and 5.06% (as %RSD) for CV and DPV, respectively.

Disulfoton-molecularly imprinted sensor (disulfoton-MIP sensor)

Computational approach for the selection of functional monomers

In order to improve the detection sensitivity of the electrochemical method for disulfoton, we next considered the use of a molecularly imprinted polymer. As the first step in the production of MIPs is the formation of a complex between template and the suitable functional monomer, the selection of the appropriate monomers is an important factor for MIP design [24]. In this work, seven functional monomers involving phenol (Ph), pyrrole (Py), Gallic acid (GA), 2-aminophenol (OAP), 2,2 Dithiodianiline (DTDA), 3,4 Ethelenedioxythiophen (ETOP), o-Phenylenediamine (OPD)] were screened computationally

for a match with the target template. These monomers are all conductive and have been selected from the literature as it is proven they are electrochemically polymerizable onto an electrode surface. One chemical structure for each monomer was separately matched with a disulfoton molecule using DFT at B3LYP level in vacuum and the calculated energy (E), shown in Table 1. The binding energy of template-monomer complex, ΔE, was calculated according to equation (4) [20]:

$$\Delta E = E(\text{template–monomer}) - E(\text{template}) - \sum E\ (\text{monomer}) \quad (4)$$

Theoretically, the most suitable monomer for preparing a MIP will have the highest stability, hence the more negative energy binding value, in the monomer-template interaction [20, 25]. Table 1 shows disulfoton-Ph has the highest -ΔE value indicating Ph has a strong interaction with disulfoton template while GA-disulfoton interaction is the weakest, for example. Therefore, Ph was selected as best monomer for designing an MIP for disulfoton.

Table 1**:** Binding energy of disulfoton and monomers (Py; Pyrrole, Ph; Phenol, OAP, O-aminophenol, OPD; 0-phenelendiamine, GA; Gallic acid , DTDA; 2,2 Dithiodianiline, EDOT; 3,4 ethelenedioxythiophen).

Monomers	E (disulfoton Monomer)	E (disulfoton)	E(Monomer)	ΔE (KJ)
Py	-2212.90512	-2002.73085	-210.16588	-0.0083
Ph	-2310.20656	-2002.73085	-307.46491	-0.0107
OAP	-2212.90512	-2002.73085	-362.81867	-0.0106
OPD	-2345.69125	-2002.73085	-342.95536	-0.0050
GA	-2649.20842	-2002.73085	-646.4739	-0.0036
DTDA	-3373.13087	-2002.73085	-1370.3911	-0.0088
EDOT	-2783.58066	-2002.73085	-780.84044	-0.0093

Fabrication of the disulfoton imprinted sensor

The optimum number of cycles on the glassy carbon surface will produce a fairly homogeneous porous molecular imprinted polymer (Fig 4A). During the electro-

polymerization of Ph in $NaClO_4$, the oxidation of Ph occurred at 0.98 V in the first cycle and the oxidation peak positively shifted and progressively decreased on subsequent cycles, indicating the polymeric film growth on the working electrode [26] (Fig 4B). When comparing the NIP, the oxidation of Ph was delayed to potential 1.02 V. As it has been noted, reversible interactions between the disulfoton molecule and the insoluble Ph polymer network were formed in the imprinting film. The oxygen and/or sulfur in the disulfoton molecules interact with the hydrogen of the hydroxyl group in the polymer through hydrogen bonding and other possible non-covalent inter-molecular interactions. The formation of this complex will define the size and orientation of the chemical functions of the imprinted cavity, which will be specific to the target analyte after removal.

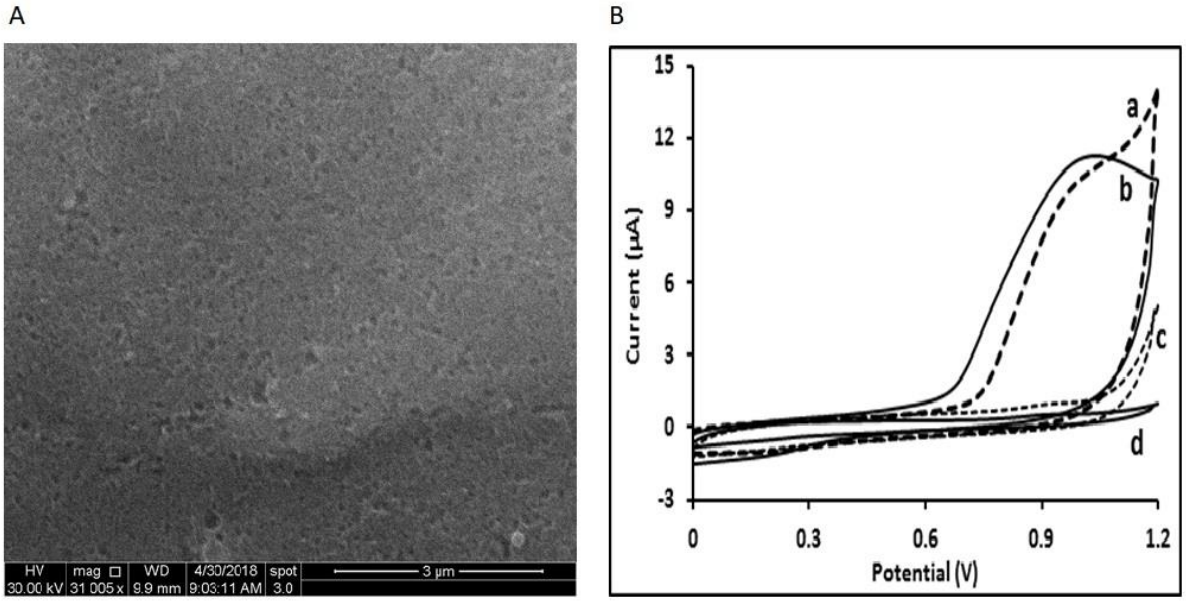

Figure 4. (A) SEM picture of the surface of the modified carbon electrode with the phenol MIP. Magnification 31005x, 30kV, 3 µm, spot 3.0, WD 9.9 mm. (B). Cyclic voltammograms obtained during the preparation of the DSN-imprinted and non-printed PolyPhenol films at GC electrode; (a) MIP at first cycle (dashed line); (b) NIP at first cycle (solid line); (c) MIP after 10 cycles (dashed line); (d) NIP after 10 cycles (solid line). Experimental conditions: [Ph] = 10mM; [DSN] = 2mM; scan rate = 50 mV/s; [$NaClO_4$] = 0.1 M; number of cyclic scans = 10

The developed MIP electrochemical sensor was tested with reference to the bare glassy carbon electrode (Fig 5). The intensity of the MIP peak was found to be greater than that of the bare GC electrode using the same concentration, suggesting the MIP sensor is more sensitive than bare electrode due to a pre-concentration effect of the MIP.

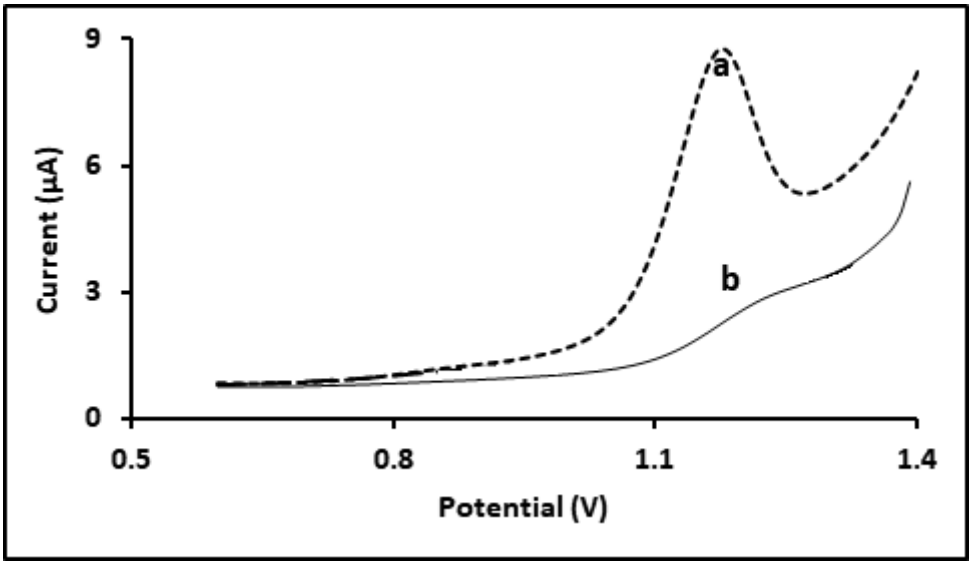

Figure 5: Differential pulse voltammetry of 25µM disulfoton in NaClO4 solution a) on disulfoton-MIP sensor and b) on bare GC electrode under optimum conditions.

When designing molecular imprinted polymers there is the possibility of non-specific interactions or some signal coming from the analyte of interest on the surface of the non-imprinted polymer (NIP). When correctly optimized these should be minimum or non-existing. In the case of the DSN-MIP these were found to be minimum as can be seen in Figure 6.

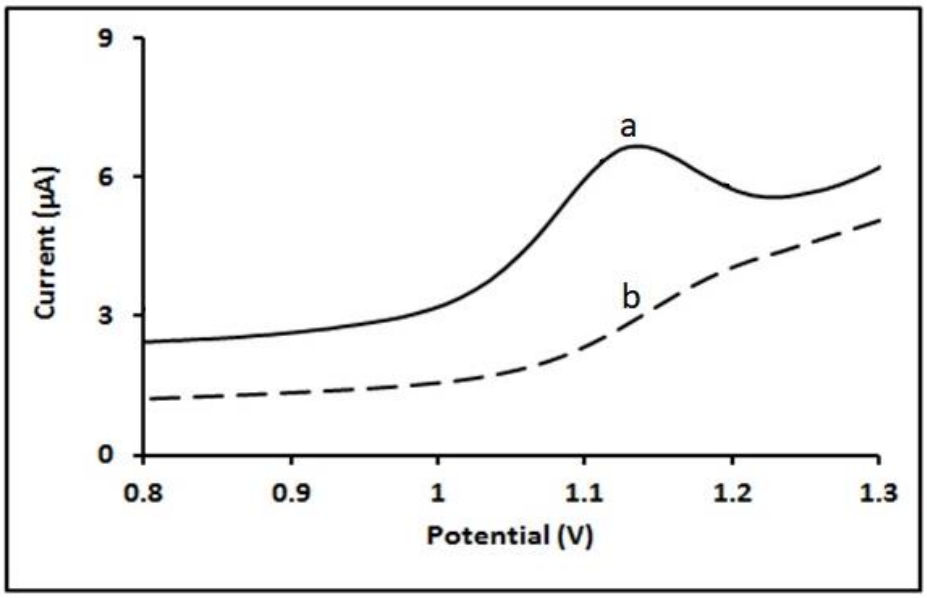

Figure 6. Differential pulse voltammetry of 30μM DSN in NaClO4 solution a) on DSN-MIP sensor, b) on NIP/GC electrode.

Optimization of the imprinted sensor

In the preparation of an imprinted sensor some factors play an important role: the concentration of the functional monomer, the template concentration and the number of scanning cycles. Theoretically, the concentration of the monomers should be higher than that of the template and an excess will affect the sensitivity of the formed MIP. [27, 28] In this way, the disulfoton-Ph molar ratio was computationally optimized using a Semi-empirical (PM3) calculation in vacuum. The calculated binding energy results are different from those of the DFT model, as expected, as they use different assumptions and give a relative (not absolute values) indication of the energy obtained for the ratio under study.

In the energy binding calculations various molar ratio of disulfoton:Ph including 1:1, 1:2. 1:3, 1:4, 1:5 and 1:6 were used. The results in Table 2 showed that the disulfoton: Ph (1:5) ratio had the highest binding energy (-23.50 kJ mol^{-1}) and the highest stability for MIP formation

[19]. Therefore, the optimal concentrations 5 M concentration of Ph and 1 M concentration of disulfoton were chosen for electro polymerization mixture.

Table 2. Binding energy of DSN: Ph ratio using Semi-Empirical calculation.

DSN:Ph (Mol)	E(DSN-Ph)	E (DSN)	E(Ph)	ΔE (KJ mol^{-1})
1:1	-573.2243	-492.8974	-90.67410	-10.3472
1:2	-684.3667	-492.8974	-203.4887	-12.0194
1:3	-789.3645	-492.8974	-303.0990	-6.6319
1:4	-869.2372	-492.8974	-397.0357	-20.6959
1:5	-936.5571	-492.8974	-467.1525	-23.5028
1:6	-1041.243	-492.8974	-556.1676	- 7.8215

After this, the number of scanning cycles was also optimized. The number of scanning cycles during the electro polymerization can control the thickness of the polymer film [27]. Generally, a thicker film will be of benefit as more imprinted sites can be produced. However, if the film is too thick, the template molecule cannot be completely removed from the polymer. This adversely affects performance and sensitivity as the disulfoton target molecules will have difficulty accessing the electrode surface leading to poor or no signal. In this study different scanning cycles, including 3 cycle, 7 cycles, 10 cycles, 15 cycles and 20 cycles, were studied. It was found that the 10 cycles polymerization produced the highest current response for the imprinted sensor.

MIP/disulfoton Sensor voltammetry

The voltammetric response of the developed MIP-disulfoton sensor was studied in $NaClO_4$ solutions; the peak current was increased with increasing concentrations of disulfoton and monitored by DPV (Fig.7). The peak currents were proportional to the concentration of

disulfoton in the range of 1-30 µM. There was a good linearity in the range of concentrations studied with a correlation coefficient r^2= 0.9985. Limit of detection and quantitation were also calculated with values of 0.183 µM and 0.6 µM, respectively, suggesting the developed sensor is ten times more sensitive than the bare GC electrode.

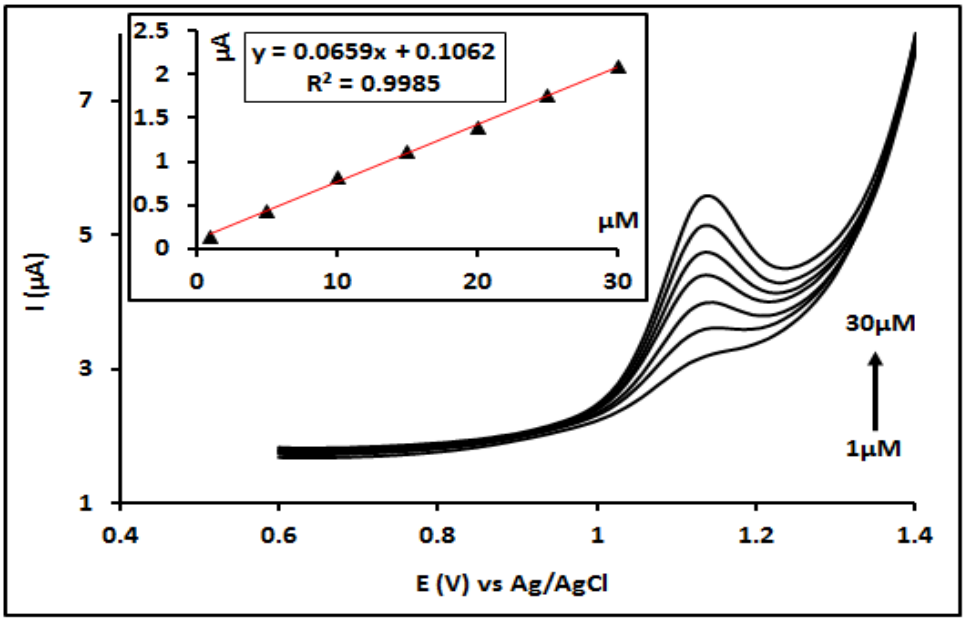

Figure 7: Differential pulse voltagramm for disulfoton at 1, 5, 10, 15, 20, 25, and 30 µM at MIP modified glasy carbon electrode. Inset: regression line for calibrated disulfoton concentrations. A pulse amplitude of 50 mV; pulse time of 40 mS; and sweep rate of 25 mV s^{-1} were used.

Precision and recovery

The precision of the disulfoton anodic peak at the GC electrode and at the developed MIP sensor were calculated as the percentage relative standard deviation (%RDS) for 5 repeated measurements on the same day (intra-day precision), and also determined in five consecutive days (inter-day precision). Table 3 shows the repeatability of the imprinted electrode for disulfoton compared with those obtained for the bare GC electrode at 25 µM. In general, the precision of the DNS-MIP is better than that of the bare GC indicating that the developed sensor is both more reliable and has greater precision. The MIP sensor

exhibited high reproducibility and was very stable for at least 5 days with subsequent cycles of washing and measuring. In addition, the recovery test was carried out by spiking 25µM disulfoton in prepared samples. The same samples were also analyzed by GC-MS, used as a reference method to compare the recovery values. The results are shown in table 3.

Table 3: Precision and recovery values for 25µM disulfoton for the electrochemical and GC-MS (reference) methods.

Method	**GC (CV)**	**GC (DPV)**	**MIP/DSN (DPV)**	**GC-MS**
Spiked Concentration (µM)	25	25	25	25
Recovered Concentration (µM)	23.20	25.60	24.97	25.50
Recovered percentage (%)	92.9	102	99.9	102
Intra-day precision (n=5), (%)	2.68	4.91	1.95	5.52
Inter-day precision (n=5), (%)	11.40	5.06	2.94	-

Application of the developed electrochemical methods in a biological matrix

To determine the validity of the proposed electrochemical methods for the determination of disulfoton in the presence of natural interfering substances, spiked human plasma and urine samples were tested. One-mL of synthetic human plasma containing DNS was added to 29mL of $NaClO_4$ solution. Accordingly, 2 mL of fresh human urine sample from a donor and spiked with DNS, was taken and diluted to 30 mL with the same solution and then directly analyzed. Known concentrations of disulfoton had been previously added to the plasma and urine samples and previously analyzed using GC-MS. Table 4 shows the results obtained from these analyses. The minimum recovered percentage was greater than 85% and 92% using the bare GC and MIP/disulfoton sensor, respectively. Thus, the results

showed that the matrix did not significantly influence the recovered concentration. Moreover, urine matrix has slightly less effect on recovered concentration than plasma.

Table 4: Recovered disulfoton using the electrochemical methods for plasma and urine samples.

Matrix Media	Applied Method	Spiked/Recovered Concentration (µM)	Recovered percentage (%)	RSD (%)
Plasma	CV (GC)	25/22.30	89.30	3.32
		35/34.70	99.30	7.88
Plasma	DPV (GC)	25/21.50	88.70	16.90
		35/35.30	101.10	8.31
Plasma	DPV (MIP/DSN)	15/14.24	94.96	4.62
		30/27.75	92.50	1.85
Urine	DPV (MIP/DSN)	15/14.69	97.96	11.39
		30/28.71	95.70	4.44
Urine	CV (GC)	25/23.60	94.56	6.64
		35/35.37	99.30	5.30
Urine	DPV (GC)	25/21.30	85.20	12.6
		35/34.20	99.10	3.10

Conclusion

It is interesting to highlight the fact that, while the utilization of MIP are getting much more attention in recent times, the design of the best polymers for selective identification of

analytes still follows a very traditional approach. Computational methods are underutilized despite the fact that these models have been around for over a decade [29]. In this paper, a highly selective electrochemical method for the measurement of disulfoton in different biofluids has been demonstrated. An oxidation peak for DNS at 1.135 V was found using a bare GC electrode by cyclic voltammetry and differential pulse voltammetry. The method showed very good linearity and a reliable precision and recovery. Using density functional theory (DFT) and semi-empirical models (PM3), a computation approach was used to design optimize a molecularly imprinter polymer for further improved of the disulfoton sensor. The best matching monomer was found to be phenol. An optimal ratio of 1:5 of template to monomer for fabrication the MIPs was also determined. Glassy carbon working electrode s were modified by electro-polymerization with the optimized monomer-template mixture using CV. The developed sensor showed an improved analytical response towards disulfoton compared to that obtained by the GC electrode. Sensitivity, selectivity, recovery and repeatability were also investigated for the developed methods in biological samples showing a good response. The obtained percentage of recovery showed good agreement compared to those reference values when GC-MS was used as a reference method.

Acknowledgement:

The authors gratefully acknowledge the financial support of this work by the Higher Committee for Educational Development, Iraq.

References:

[1] Q. Gan, U. Jans, *J. Agric. Food Chem* **2006**, 54, 7753-7760.

[2] A. Bavili Tabrizi, A. Abdollahi, *Bull. Environ. Contam. Toxicol* **2015**, 95, 536-541.

[3] A.M. Faria, R.P. Dardengo, C.F. Lima, A.A. Neves, M.E.R. Queiroz, *Intern. J. Environ. Anal. Chem.* **2007**, 87, 249-258.

[4] K. Usui, Y. Hayashizaki, T. Minagawa, M. Hashyada, A. Nakano, M. Funayama, *Leg. Med.* **2012**, 14(6), 309-316.

[5] Agency for Toxic Substances and Disease Registry (ATSDR). Addendum to the toxicological profile for disulfoton, US department of health and human services: Atlanta, Georgia, 2011.

[6] Agency for Toxic Substances and Disease Registry (ATSDR). Toxicological profile for disulfoton, US department of health and human services: Atlanta, Georgia, 1995.

[7] M. Catala-Icardo, L. Lahuerta-Zamora, S. Torres-Cartas, S.J. Meseguer-Lloret, *J. Chromatogr. A* **2014**, 1341, 31-40.

[8] P.S. Chen, S.D. Huang, *Talanta* **2006**, 69, 669-675.

[9] M.C. Henderson, S.K. Krueger, L.K. Siddens, J.F. Stevens, D.E. Williams, *Biochem. Pharmacol.* **2004**, 68, 959-967.

[10] S.A. Piletsky, S. Alcock, A.P. Turner, *Trends Biotechnol.* **2001**, 19, 9-12.

[11] E.L. Holthoff, F.V. Bright, *Anal. Chim. Acta* **2007**, 594, 147-161.

[12] S.A. Piletsky, A.P. Turner, *Electroanalysis* **2002**, 14, 317-323.

[13] Z. Zhao, Y. Teng, G. Xu, T. Zhang, X. Kan, *Anal. Lett.* **2013**, 46, 2180–2188.

[14] S.K. Mamo, J. Gonzalez-Rodriguez, *Sensors* **2014**, 14, 23269-23282.

[15] T. Alizadeh, A. Akbari, *Biosens. Bioelectron*. **2013**, 43, 321-327.

[16] J. Luo, C. Fan, X. Wang, R. Liu, X. Liu, *Sens. Actuators B*, **2013**, 188, 909-916.

[17]I.M. Baldim, M.C. Souza, J.C. Souza, E.C. Figueiredo, I. Martins, *Anal. Bioanal. Chem*, **2012**, 404, 1959-1966.

[18] S. Pardeshi, R. Dhodapkar, A. Kumar, *Spectrochim. Acta, Part A*. **2013**, 116, 562-573.

[19] K.K. Tadi, R.V.J. Motghare, *Chem. Sci.* **2013**, 125, 413-418.

[20] A. Nezhadalia, M. Mojarrab, *Sens. Actuators B* **2014**, 190, 829-837.

[21] B. Qader, M.G. Baron, I. Hussain, J.Gonzalez-Rodriguez, *J. Electroanal. Chem.* **2018**, 821, 16-21.

[22] T. Sarigül, R. Inam, H.Y. Aboul-Enein, *Talanta* **2010**, 82, 1814-1819.

[23] E.J. Laviron, J. *Electroanal. Chem* **1979**, 101, 19-28.

[24] B.S. Batlokwa, Development of molecularly imprinted polymer based solid phase extraction sorbents for the selective clean-up of food and pharmaceutical residue samples.: Rhodes University, 2011.

[25] M.B. Gholivand, M. Khodadian, F. Ahmadi, *Anal. Chim. Acta* ***2010***, 658, 225-232.

[26] N.B. Tahar, A.J. Savall, *Appl. Electrochem*, **2011**, 41, 983-989.

[27] H. Hrichi, M.R. Louhaichi, L. Monser, N. Adhoum, *Sens. Actuators, B* **2014**, 204, 42-49.

[28] B. Schweiger, J. Kim, Y.J. Kim, M. Ulbricht, *Sensors*, **2015**, 15, 4870-4889.

[29] Yolanda Diñeiro, M. Isabel Menendez, M. Carmen Blanco-Lopez, M. Jesus Lobo-Castañon, Arturo J. Miranda-Ordieres, and Paulino Tuñon-Blanco, Anal Chem. **2005**, 77, 6741-6746.